

# Resolving vertical tectonics in the San Francisco Bay Area from permanent scatterer InSAR and GPS analysis

Roland Bürgmann Department of Earth and Planetary Science and Berkeley Seismological Laboratory, University of California, Berkeley, California 94720, USA

George Hilley Department of Geological and Environmental Sciences, Stanford University, Stanford, California 94305, USA  
Alessandro Ferretti }  
Fabrizio Novali } Tele-Rilevamento Europa, Via Vittoria Colonna 7, 20149 Milan, Italy

## ABSTRACT

Using a combination of GPS-measured horizontal velocities of 200 sites and 115,487 range-change rates determined with the permanent scatterer interferometric synthetic aperture radar (InSAR) method in the San Francisco Bay Area, we resolve vertical motions in the region at sub-mm/yr precision. The highest displacement rates are due to nontectonic processes, such as active landslides, subsidence and rebound over aquifers, and rapid settling of unconsolidated sediments along the bay margins. Residual displacement rates are determined by removing the contribution of the GPS-derived horizontal velocity field from the InSAR range-change rates. To isolate vertical tectonic rates, we use only those InSAR measurements made on material that was not Quaternary substrate, which is susceptible to nontectonic and seasonally varying ground motions. The InSAR residuals indicate significant uplift over the southern foothills of the active Mount Diablo anticlinorium, the Mission Hills stepover region of the Hayward and Calaveras faults, and the central and southern Santa Cruz Mountains located along a restraining bend of the San Andreas fault.

**Keywords:** geodesy, San Andreas fault, uplifts, San Francisco Bay region, GPS.

## INTRODUCTION

The San Andreas fault system in central California is a transform plate boundary accommodating  $\sim 38$  mm/yr of right-lateral motion between the Pacific plate and the Sierra Nevada–Great Valley block (Argus and Gordon, 2001; d’Alessio et al., 2005). Regional contraction across the San Andreas fault system has occurred at rates of  $\sim 1$ – $5$  mm/yr since 3–5 Ma (Argus and Gordon, 2001). In addition to deformation associated with regional plate-normal convergence, high rates of shortening accommodated by thrust faulting occur in areas of restraining strike-slip fault geometries. In the San Francisco Bay Area, an  $\sim 10^\circ$  bend of the San Andreas fault through the Santa Cruz Mountains, the Mission Hills stepover region between the Calaveras and Hayward faults, and a left stepover between the Greenville and Concord faults (encompassing the Mount Diablo anticlinorium) are areas of localized contraction and high topography (Fig. 1). Here, we use a new approach that allows us to determine a detailed image of vertical motions from nontectonic and tectonic processes by combining precise but sparsely distributed GPS-site motions with a large data set of satellite-to-ground range changes measured with interferometric synthetic aperture radar (InSAR).

## SURFACE DEFORMATION MEASUREMENTS

Except for the coseismic and postseismic effects of large earthquakes, the active defor-

mation rates in the San Francisco Bay Area appear to have been constant (Bürgmann et al., 1997; Lisowski et al., 1991; Savage et al., 1994). A record of GPS acquisitions, now more than ten years’ worth, provides precise horizontal site velocities and reveals the nature of elastic strain accumulation about the major strands of the San Andreas fault system (d’Alessio et al., 2005). However, GPS is not able to resolve the low interseismic uplift rates that may be associated with the contractional structures in the Bay Area (Bürgmann et al., 1994). Historic leveling measurements provide limited information about possible tectonic uplift in the eastern Bay Area (Gilmore, 1993). InSAR has revealed centimeter-level uplift and subsidence patterns related to the seasonal drawdown and recharge of the Santa Clara Valley aquifer (Schmidt and Bürgmann, 2003), rapid motions of deep-seated landslides (Hilley et al., 2004), and a possible sub-mm/yr contribution of an east-side-up, dip-slip component to the range-change offset across the creeping northern Hayward fault (Hilley et al., 2004; Schmidt et al., 2005).

InSAR only provides a one-dimensional measurement of change in distance along the look direction of the radar spacecraft, but is highly sensitive to vertical motion due to its steep (here  $20^\circ$ – $26^\circ$  off-vertical) look angle (Bürgmann et al., 2000). InSAR measurements that rely on one or a stack of several interferograms are often hampered by significant noise introduced by atmospheric delays

and by loss of coherence in vegetated or high-relief terrain. A new InSAR processing technique, the permanent scatterer-interferometric synthetic aperture radar (PS-InSAR) method (Colesanti et al., 2003; Ferretti et al., 2000, 2001), allows for the identification and integration of individual radar-bright and radar-phase-stable points (outcrops, buildings, utility poles, etc.) in more than 15 SAR images. The phase data from these permanent scatterers are then used to separate time-dependent surface motions, atmospheric delays, and elevation-error components of the range-change measurement (Colesanti et al., 2003). We incorporate 49 European Remote Sensing satellite (ERS-1 and ERS-2) acquisitions collected from 1992 to 2000 of our Bay Area target scene (track 70, frame 2853) (Fig. 1). Points whose displacements vary in a highly nonlinear fashion, such as a large area of rapid seasonal uplift and subsidence in the Santa Clara Valley (Colesanti et al., 2003; Schmidt and Bürgmann, 2003), are excluded from the final data set. The PS-InSAR data provide range-change rates at 115,487 points, including targets in vegetated or mountainous areas that are unsuitable for standard InSAR. In addition, this data set contains a time series of displacement, which allows us to identify regions in which there is a significant time-dependent, often seasonal component to the deformation field.

## RESOLVING VERTICAL TECTONICS

Range-change rates recorded by the PS-InSAR measurements include the contribution of horizontal tectonic motions that project into the radar line-of-sight vector. To isolate the vertical component of the deformation, we use the GPS-derived horizontal velocity field to eliminate its contribution to each PS-InSAR range-change measurement. To this end, we use a 200-station subset of a regional 1993–2004 GPS velocity field (d’Alessio et al., 2005) to constrain a mechanical model of the horizontal deformation field. In the model, uniform-slip dislocations in an elastic half-space (Okada, 1985) reproduce the surface strain field about the Bay Area faults. Interseismic shear about a locked strike-slip fault is approximated by slip on a buried vertical screw dislocation extending deep below the

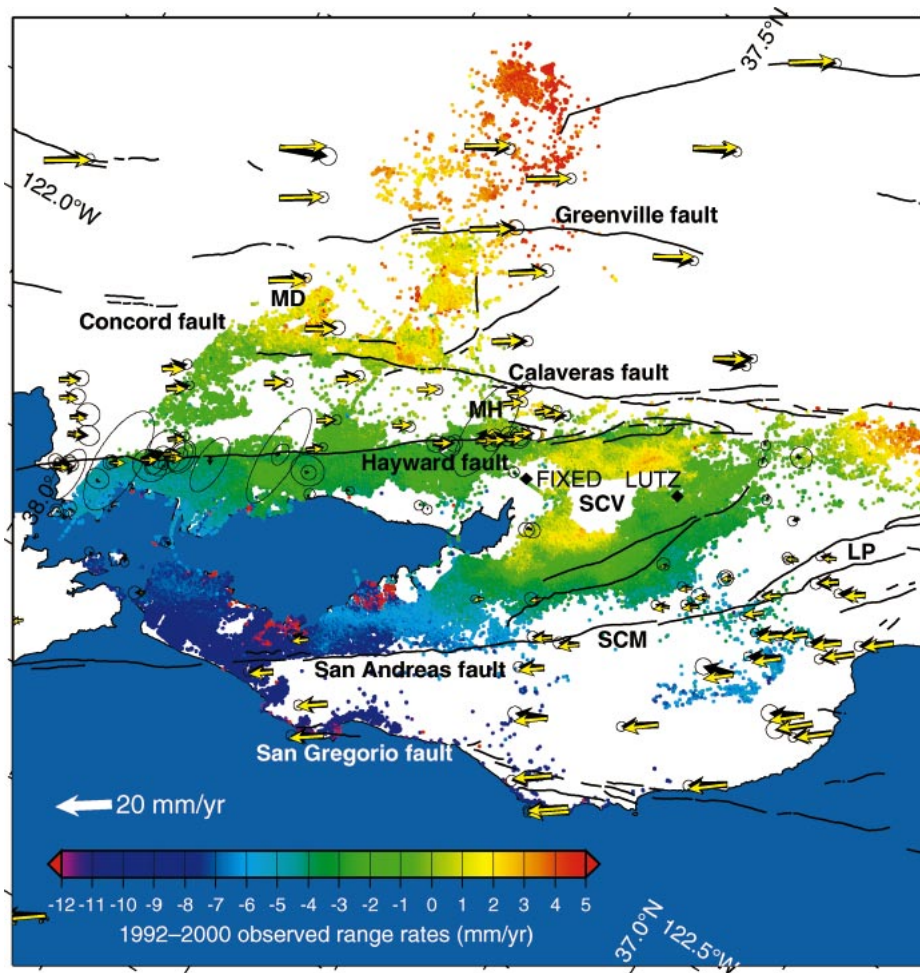


**Figure 1.** Fault map of San Francisco Bay Area in oblique Mercator projection about pole of Pacific plate to Sierra Nevada–Great Valley (SNGV) block rotation (d’Alessio et al., 2005). We include 1993–2003 GPS velocities (black arrows tipped with 95% confidence ellipses, not all in map frame; Table DR2 [see footnote 1]) relative to central bay station LUTZ. Yellow arrows are predicted velocities calculated from dislocation model (model parameters in Table DR1). Color-scaled dots show 1992–2000 PS-InSAR range-change rates of 115,487 permanent scatterers relative to point labeled FIXED. LP—Loma Prieta; MD—Mount Diablo; MH—Mission Hills; SCM—Santa Cruz Mountains; SCV—Santa Clara Valley.

seismogenic zone. Creep on the Hayward, southern Calaveras, and central San Andreas faults is modeled by shallow dislocation elements. A simple 17-element dislocation model (Table DR1<sup>1</sup>) can explain much of the observed horizontal displacement field. The summed misfit to the GPS velocities, the (unitless) weighted residual sum of squares (*WRSS*), of this model is 1173, and the reduced misfit statistic  $\sqrt{WRSS/(n-p)}$  is 3.1, where *n* and *p* are the number of data (199 north and east velocities relative to reference station) and model parameters (strike slip on 17 dislocations), respectively. The only large

<sup>1</sup>GSA Data Repository item 2006041, model parameters (Table DR1), GPS data (Table DR2), and Figs DR1 and DR2, is available online at [www.geosociety.org/pubs/ft2006.htm](http://www.geosociety.org/pubs/ft2006.htm), or on request from [editing@geosociety.org](mailto:editing@geosociety.org) or Documents Secretary, GSA, P.O. Box 9140, Boulder, CO 80301-9140, USA.

area that exhibits a systematic misfit pattern in the residual GPS velocities lies along the Loma Prieta section of the San Andreas fault, where a region of apparent residual contraction and right-lateral shear of  $\leq 5$  mm/yr is observed. The remaining high residuals either are apparent outliers or are located along creeping fault segments where more detailed, slip-distributed models are appropriate (Schmidt et al., 2005).

We use the modeled horizontal velocity field to calculate predicted range-change rates along the individually computed line-of-sight vectors due to horizontal motions at each InSAR data point (Fig. DR1). The modeled rates are then subtracted from the observed PS-InSAR rates. As the PS-InSAR range-change field may include a small contribution from remaining satellite orbit-baseline errors, we also estimate and remove the contribution of a small regional linear range-change gra-

dient (of 0.094 mm/km) across the scene determined in a joint inversion of both data sets. Scatter in the data at the level of about  $\pm 0.5$  mm/yr is probably in large part due to the inherent instability of the objects that reflect radar, which mostly consist of built structures.

Residual range-change rates represent the combined effects of horizontal and vertical motions that are unaccounted for by the tectonic dislocation model. Where nontectonic horizontal displacement rates are small and the simplified velocity field produced by the dislocation model adequately represents the actual tectonic velocity field, the residual range-change rates may be interpreted in terms of vertical motions. In this case, the inferred vertical displacement rates are 1.08–1.10 times the residual range-change rate, a factor that slightly varies with the look angle across the area.

## RESULTS AND INTERPRETATIONS

When the range-change contribution due to horizontal tectonic motions (Fig. DR1; see footnote 1) is removed from the data, we find that the largest motions revealed in the PS-InSAR data are due to various nontectonic hydrological and surface processes (Fig. DR2). Many of the nontectonic features are highly localized, including active landslides (Hilley et al., 2004) and localized subsidence along the bay due to consolidation of man-made fill and bay mud (Ferretti et al., 2004). Regions of uplift overlie young sedimentary basins that are expanding due to increasing groundwater levels during the observation period (Schmidt and Bürgmann, 2003).

To resolve tectonic deformation, we identify points in the data set in which these nontectonic processes severely influence the deformation measurement. The PS-InSAR data suggest that points located on Quaternary substrate are generally more likely to record deformation related to nontectonic processes, and so we use a GIS-produced map of the distribution of Quaternary units in the region (Knudsen et al., 2000) to separate 92,102 points located on Quaternary units from those on bedrock (i.e., non-Quaternary) (Fig. 2). In addition, we analyze the time series of all PS-InSAR points to identify points that show strong seasonal deformation (Fig. 3). We find that points within bedrock units display long-term vertical displacement rates ( $\leq 2$  mm/yr, Fig. 2) that are far smaller than points on Quaternary substrate with rates up to  $\sim 10$  mm/yr (Fig. DR2).

Interestingly, even PS-InSAR points presumably located on bedrock show substantial seasonal fluctuations that often appear coherent over large areas (Fig. 3). Pre-Quaternary units may experience some hydrologic expansion or contraction and can be mantled with unstable soils. However, the bedrock points’



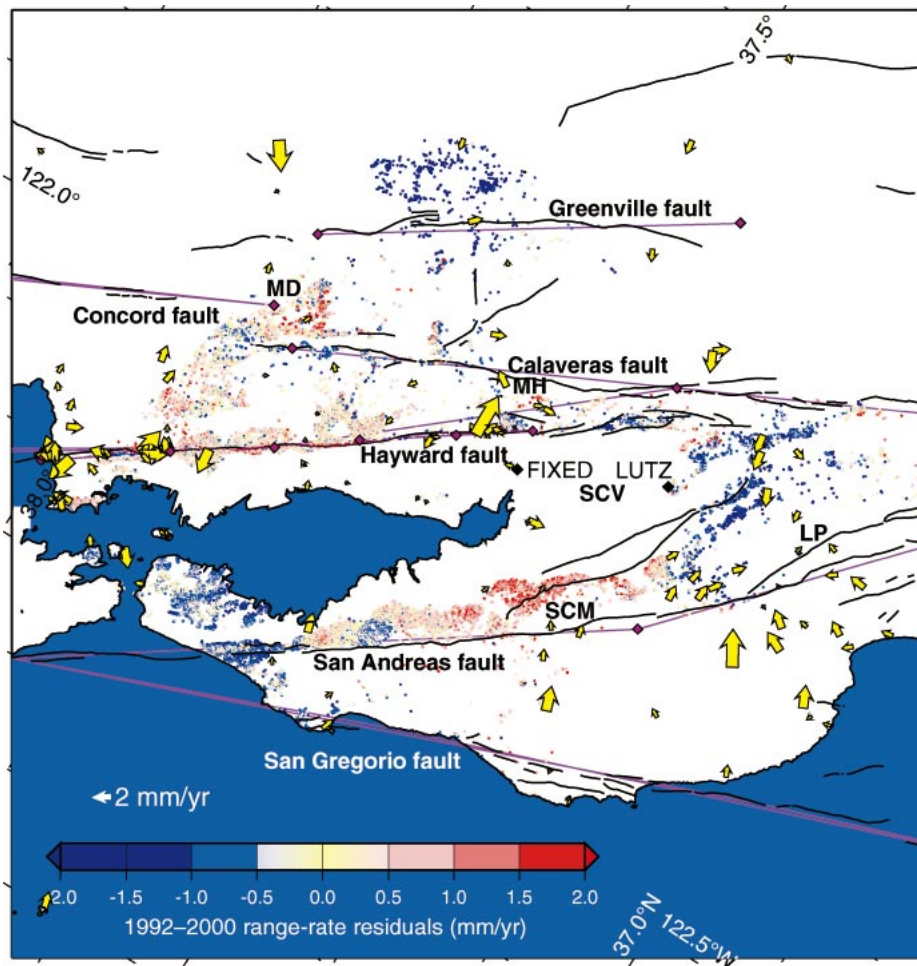


**Figure 2.** Residual PS-InSAR rates after removing contribution of tectonic horizontal motions and all points located on Quaternary substrate. Inferred uplift rates are 1.08–1.10 times the range-change rates depicted, assuming that all remaining deformation is due to vertical motions (positive range-rate residuals correspond to uplift). Yellow arrows are GPS residual (observed minus modeled) horizontal velocities, and pink lines and diamonds are vertical model dislocation planes and their ends, respectively. Abbreviations are as in Figure 1.

magnitude and sign of the seasonal vertical displacement often change over several seasons, while points lying on Quaternary substrate consistently subsided during the dry season and rebounded during the wet season. The amplitude of seasonal fluctuations tends to be ~2–3 times larger for the Quaternary PS-InSAR points than for bedrock points (Fig. 3).

When interpreted in terms of vertical motions, the residual range-change rate field of bedrock target points includes three larger areas of subsidence and three regions of uplift at 0.5–1.5 mm/yr rates (Fig. 2). One area of apparent subsidence is located east of the Greenville fault, and we have no obvious explanation for this feature. The second area of subsidence at rates of up to ~2 mm/yr appears localized about the epicentral region of the 1989,  $M_w = 6.9$ , Loma Prieta earthquake and coincides with the region of horizontal contraction evident in the residual GPS velocities. The direction and magnitude of these residual

horizontal velocities can explain only ~0.5 mm/yr of the residual range-change rate, and subsidence at ~1.5 mm/yr is indicated. Such subsidence is expected due to continued postseismic relaxation at depth following the Loma Prieta earthquake (Pollitz et al., 1998). A third zone of slow (~0.5 mm/yr) subsidence along the northern San Francisco peninsula may be related to an extensional bend in the San Andreas fault and/or interaction with the offshore San Gregorio fault zone.

Uplift rates on the order of 1 mm/yr are indicated along the southern Santa Cruz Mountains that flank Santa Clara Valley, along the peak elevations of the Mission Hills, and within the southern foothills of Mount Diablo. Inferred uplift is observed on both sides of the San Andreas fault between 37°10'N and 37°30'N, but appears to be highest to the northeast overlying a number of Quaternary thrust faults (Bürgmann et al., 1994). As the Santa Cruz Mountains uplift zone is adjoined by the rapidly expanding Santa Clara aquifer,

we are not able to fully characterize the shape of the uplift zone or develop a well-constrained mechanical model of the deformation. The uplift is terminated to the southeast by the Loma Prieta zone of subsidence and residual contraction. Overall, the data suggest that uplift occurs over a broad zone, consistent with regional contraction along the restraining bend in the San Andreas fault that is ultimately accommodated by discrete thrust faulting and folding.

Points located between the Hayward and Calaveras faults appear to be rising at rates of 0–1.5 mm/yr. The highest uplift rates are localized in a small zone coinciding with the highest elevations of the Mission Hills (Fig. 2). Relocated seismicity and focal mechanisms in the stepover region indicate oblique right-lateral slip on a steeply northeast-dipping fault (Manaker et al., 2005). Abundant microseismicity and observation of repeating small earthquakes along this fault at 5–10 km depth (Schmidt et al., 2005) suggest that aseismic fault creep occurs at least over that depth range and may explain the localized nature of the high uplift rates.

## DISCUSSION AND CONCLUSIONS

Our study shows how contributions from nontectonic processes and time-dependent earthquake cycle deformation make the identification and interpretation of active, vertical tectonics from geodetic measurements a challenging endeavor. The largest vertical motions are due to nontectonic processes such as landsliding, seasonal and long-term groundwater-level changes, and sediment settling. If we exclude all data points located on Quaternary substrate to limit contributions to the deformation signal from nontectonic motions, the InSAR range-change rates corrected for horizontal tectonic motions reflect vertical deformation rates in the region that are <2 mm/yr. The range-change time series of bedrock points appear to also contain seasonal variations due to hydrologic or atmospheric processes, which are superimposed over the long-term uplift patterns we infer over eight years of PS-InSAR observations. Thus, it is important to establish a long-term (i.e., decadal) record of vertical motions to obtain reliable measures of tectonic uplift and subsidence. The joint use of continuous GPS and multiple PS-InSAR data sets obtained from different acquisition geometries and radar satellites will allow for future improvements in the accuracy of space-geodetic uplift measurements.

The highest uplift rates appear to coincide with known areas of folding and thrusting related to restraining fault bends and stepovers along the Bay Area strike-slip faults. These include the southern foothills of the Mount Diablo fold and thrust belt, the stepover region between the Hayward and Calaveras faults,

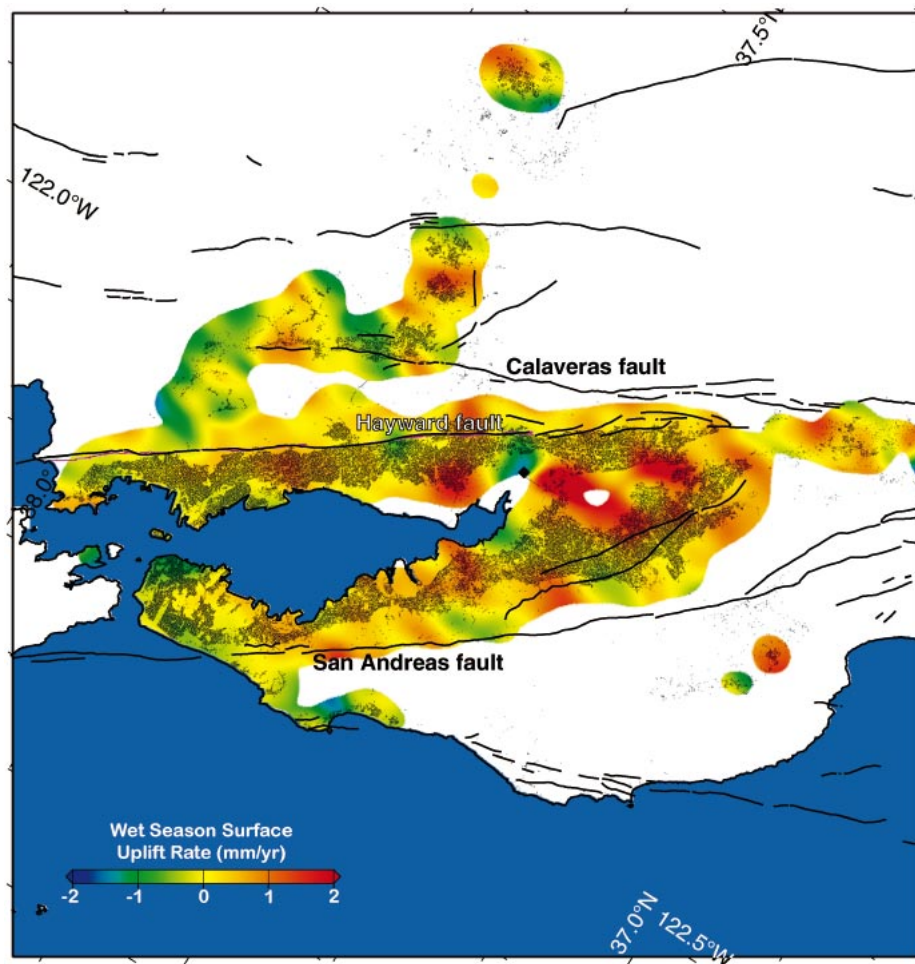


**Figure 3.** Magnitude of coherent, seasonal fluctuations in range-change time series of all permanent scatterer—interferometric synthetic aperture radar (PS-InSAR) data points. The long-term rates are removed from time series, and dry-to-wet season motions from 1996 to 2000 are stacked and filtered using a Gaussian filtering algorithm with smoothing radius of 2.8 km to highlight spatial correlation in seasonal range-change variations. Gray dots indicate PS-InSAR data points located on Quaternary substrate.

and the Santa Cruz Mountains northwest of the Loma Prieta epicentral region. Active uplift rates of  $\sim 1$  mm/yr in these regions suggest rapid convergence rates and potentially significant earthquake hazard associated with the underlying active thrust faults.

#### ACKNOWLEDGMENTS

Eric Fielding, Rob Mellors, and an anonymous reviewer provided valuable reviews. Tim Wright provided a program for calculating the line-of-sight vectors. SAR data were provided to the WInSAR Consortium by the European Space Agency (ESA) through Eurimage. Supported by U.S. Geological Survey NEHRP External Program grant 05HQGR0038. Berkeley Seismolab Contribution #05-012.

#### REFERENCES CITED

Argus, D., and Gordon, R., 2001, Present tectonic motion across the Coast Ranges and San Andreas fault system in central California: *Geological Society of America Bulletin*, v. 113, p. 1580–1592, doi: 10.1130/0016-7606(2001)113<1580:PTMATC>2.0.CO;2.

Bürgmann, R., Arrowsmith, R., Dumitru, T., and McLaughlin, R., 1994, Rise and fall of the

southern Santa Cruz Mountains, California, deduced from fission track dating, geomorphic analysis, and geodetic data: *Journal of Geophysical Research*, v. 99, p. 20,181–20,202, doi: 10.1029/94JB00131.

Bürgmann, R., Segall, P., Lisowski, M., and Svarc, J., 1997, Postseismic strain following the 1989 Loma Prieta earthquake from GPS and leveling measurements: *Journal of Geophysical Research*, v. 102, p. 4933–4955, doi: 10.1029/96JB03171.

Bürgmann, R., Rosen, P.A., and Fielding, E.J., 2000, Synthetic aperture radar interferometry to measure Earth's surface topography and its deformation: *Annual Review of Earth and Planetary Sciences*, v. 28, p. 169–209, doi: 10.1146/annurev.earth.28.1.169.

Colesanti, C., Ferretti, A., Novali, F., Prati, C., and Rocca, F., 2003, SAR Monitoring of progressive and seasonal ground deformation using the permanent scatterers technique: *IEEE Transactions on Geoscience and Remote Sensing*, v. 41, p. 1685–1701, doi: 10.1109/TGRS.2003.813278.

d'Alessio, M.A., Johansen, I.A., Bürgmann, R., Schmidt, D.A., and Murray, M.H., 2005, Slicing up the San Francisco Bay area: Block kinematics and fault slip rates from GPS-derived surface velocities: *Journal of Geophysical Research*, v. 110, B06403, doi: 10.1029/2004JB003496.

search, v. 110, B06403, doi: 10.1029/2004JB003496.

Ferretti, A., Prati, C., and Rocca, F., 2000, Nonlinear subsidence rate estimation using permanent scatterers in differential SAR interferometry: *IEEE Transactions on Geoscience and Remote Sensing*, v. 38, p. 2202–2212, doi: 10.1109/36.868878.

Ferretti, A., Prati, C., and Rocca, F., 2001, Permanent scatterers in SAR interferometry: *IEEE Transactions on Geoscience and Remote Sensing*, v. 39, p. 8–20, doi: 10.1109/36.898661.

Ferretti, A., Novali, F., Bürgmann, R., Hilley, G., and Prati, C., 2004, InSAR permanent scatterer analysis reveals ups and downs in the San Francisco Bay area: *Eos (Transactions, American Geophysical Union)*, v. 85, p. 317.

Gilmore, T.D., 1993, Historical uplift measured across the eastern San Francisco Bay region: California Division of Mines and Geology Special Publication 113, p. 55–63.

Hilley, G.E., Bürgmann, R., Ferretti, A., Novali, F., and Rocca, F., 2004, Dynamics of slow-moving landslides from permanent scatterer analysis: *Science*, v. 304, p. 1952–1955, doi: 10.1126/science.1098821.

Knudsen, K.L., Sowers, J.M., Witter, R.C., Wentworth, C.M., and Helley, E.J., 2000, Preliminary maps of Quaternary deposits and liquefaction susceptibility, nine-county San Francisco Bay region, California: A digital database: U.S. Geological Survey Open-File Report 00-444: <http://pubs.usgs.gov/of/2000/of00-444/> (November 2005).

Lisowski, M., Savage, J.C., and Prescott, W.H., 1991, The velocity field along the San Andreas fault in central and southern California: *Journal of Geophysical Research*, v. 96, p. 8369–8389.

Manaker, D.M., Michael, A.J., and Bürgmann, R., 2005, Subsurface structure and mechanics of the Calaveras Hayward fault stepover from three-dimensional vp and seismicity, San Francisco Bay region, California: *Bulletin of the Seismological Society of America*, v. 95, p. 446–470, doi: 10.1785/0120020202.

Okada, Y., 1985, Surface deformation due to shear and tensile faults in a half-space: *Bulletin of the Seismological Society of America*, v. 75, p. 1135–1154.

Pollitz, F., Bürgmann, R., and Segall, P., 1998, Joint estimation of afterslip rate and postseismic relaxation following the 1989 Loma Prieta earthquake: *Journal of Geophysical Research*, v. 103, p. 26,975–26,992, doi: 10.1029/98JB01554.

Savage, J.C., Lisowski, M., and Svarc, J.L., 1994, Postseismic deformation following the 1989 (M = 7.1) Loma Prieta, California, earthquake: *Journal of Geophysical Research*, v. 99, p. 13,757–13,765, doi: 10.1029/94JB00507.

Schmidt, D.A., and Bürgmann, R., 2003, Time-dependent land uplift and subsidence in the Santa Clara Valley, California, from a large InSAR data set: *Journal of Geophysical Research*, v. 108, 2416, doi: 10.1029/2002JB002267.

Schmidt, D.A., Bürgmann, R., Nadeau, R.M., and d'Alessio, M.A., 2005, Distribution of aseismic slip rate on the Hayward fault inferred from seismic and geodetic data: *Journal of Geophysical Research*, v. 110, B08406, doi: 10.1029/2004JB003397.

Manuscript received 24 July 2005

Revised manuscript received 16 November 2005

Manuscript accepted 18 November 2005

Printed in USA